Environmental Pollution 312 (2022) 120027

Contents lists available at ScienceDirect

Environmental Pollution

journal homepage: www.elsevier.com/locate/envpol

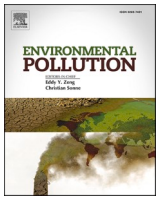

Investigating detection probability of mobile survey solutions for natural gas pipeline leaks under different atmospheric conditions☆

Shanru Tian [a], Stuart N. Riddick [b], Younki Cho [b], Clay S. Bell [b], Daniel J. Zimmerle [b,c], Kathleen M. Smits [d,*]

[a] Department of Civil Engineering, The University of Texas at Arlington, Arlington, TX, 76019, United States
[b] The Energy Institute, Colorado State University, Fort Collins, CO, 80523, United States
[c] Department of Mechanical Engineering, Colorado State University, Fort Collins, CO, 80523, United States
[d] Department of Civil and Environmental Engineering, Southern Methodist University, Dallas, TX, 75275, United States

ARTICLE INFO

Keywords:
Methane emissions
Pipeline leakage
Detection probability
Mobile survey
Atmospheric stability

ABSTRACT

The 2015 Paris agreement aims to cut greenhouse gas emissions and keep global temperature rise below 2 °C above pre-industrial levels. Reducing CH_4 emissions from leaking pipelines presents a relatively achievable objective. While walking and driving surveys are commonly used to detect leaks, the detection probability (DP) is poorly characterized. This study aims to investigate how leak rates, survey distance and speed, and atmospheric conditions affect the DP in controlled belowground conditions with release rates of 0.5–8.5 g min^{-1}. Results show that DP is highly influenced by survey speed, atmospheric stability, and wind speed. The average DP in Pasquill–Gifford stability (PG) class A is 85% at a low survey speed (2–11 mph) and decreases to 68%, 63%, 65%, and 60% in PGSC B/C, D, E/F, and G respectively. It is generally less than 25% at a high survey speed (22–34 mph), regardless of stability conditions and leak rates. Using the measurement data, a validated DP model was further constructed and showed good performance (R^2: 0.76). The options of modeled favorable weather conditions (i.e., PG stability class and wind speed) to have a high DP (e.g., >50%) are rapidly decreased with the increase in survey speed. Walking survey is applicable over a wider range of weather conditions, including PG stability class A to E/F and calm to medium winds (0–5 m s^{-1}). A driving survey at a low speed (11 mph) can only be conducted under calm to low wind speed conditions (0–3 m s^{-1}) to have an equivalent DP to a walking survey. Only calm wind conditions in PG A (0–1 m s^{-1}) are appropriate for a high driving speed (34 mph). These findings showed that driving survey providers need to optimize the survey schemes to achieve a DP equivalence to the traditional walking survey.

1. Introduction

Natural gas (NG), composed of 60–98% methane (CH_4), is considered a cleaner energy source than other fossil fuels, such as coal. NG has been promoted as a transition fuel until renewable technologies can prove greenhouse gas (GHG) emission free energy (Alvarez et al., 2012; Levi, 2013; Zhang et al., 2016; Zou et al., 2018; Zhang et al., 2022). Its use has grown rapidly and is now a significant component of the global energy resource (Heath et al., 2015; Schivley et al., 2018; Zhang et al., 2022). For example, NG provides 30% of the energy consumption in the U.S. and requires an extensive infrastructure including three million miles of NG pipeline (U.S. Energy Information Administration, 2021; National Academies of Sciences, 2022). Leak detection for pipeline systems has historically been driven primarily by concerns of public safety to reduce fatal and non-fatal incidents caused by pipeline leaks. However, more recently reducing CH_4 emissions from NG systems, including pipelines, has been identified as a way to help mitigate climate change and meet the goals of the Paris agreement (Nisbet et al., 2020).

From 2002 to 2021, the Pipeline and Hazardous Materials Safety Administration (PHMSA) reported 2986 NG pipeline incidents (153 from gathering lines, 1439 from transmission lines, and 1394 from distribution lines), resulting in 227 fatalities (38 and 189 from transmission and distribution lines, respectively) and 1030 injuries (6, 157 and 867 from gathering, transmission and distribution lines,

☆ This paper has been recommended for acceptance by Alessandra De Marco.

* Corresponding author.
E-mail address: ksmits@smu.edu (K.M. Smits).

https://doi.org/10.1016/j.envpol.2022.120027
Received 8 July 2022; Received in revised form 19 August 2022; Accepted 19 August 2022
Available online 24 August 2022

respectively) (PHMSA, 2022). Recent studies suggest that the NG supply chain system in the U.S. was responsible for 6.6 Tg of CH_4 emissions in 2020, corresponding to 0.79% of the 111.2 billion cubic feet per day (bcf day^{-1}) of NG produced (~833.45 Tg NG yr^{-1}) (U.S. Energy Information Administration, 2022; U.S. EPA, 2022). CH_4 has a global warming potential 86 times greater than that of CO_2 over a 20-year horizon (IPCC, 2014), and the environmental benefits of using NG as a near-term bridging fuel would be offset if the NG supply chain emits CH_4 more than 3.2% of the total NG production (Alvarez et al., 2012; UNFCCC, 2022). Reducing CH_4 emissions from the NG supply chain presents a relatively straightforward objective for GHG mitigation while improving public safety.

Currently, walking and driving surveys are commonly used to detect NG leaks from pipelines (Phillips et al., 2013; Gallagher et al., 2015; Zimmerle et al., 2017; Weller et al., 2018; Cho et al., 2020; Li et al., 2020; Riddick et al., 2021). In a walking survey, surveyors walk along the pipelines and detect enhanced CH_4 mole fractions using a handheld instrument, such as a Bascom-Turner Gas-Rover (GR; range: 5–10,000 ppm; accuracy: 2% ± 10 ppm; frequency: 1–2 Hz) or Heath Inc. Remote Methane Leak Detector (RMLD; range: 0–99,999 ppm-m; sensitivity: 5−10 ppm-m, frequency: 3 Hz) (Zimmerle et al., 2017; Weller et al., 2018; Cho et al., 2020; Riddick et al., 2021). GR measures the surface CH_4 mole fraction by drawing air from the surface onto a dual catalytic combustion sensor (for measuring between 0 and 2 vol % CH_4) or a thermal conductivity sensor (2–100 vol % CH_4) (Cho et al., 2020; Riddick et al., 2021). RMLD uses laser technology (Tunable Diode Laser Absorption Spectroscopy) to measure the path-integrated CH_4 mole fraction (reported as ppm-m) remotely within a 30 m distance of the pipeline (Heath Consultants, 2009). A driving survey measures the CH_4 mole fraction in the air at a distance of up to 200 m from the source using a trace gas CH_4 analyzer, such as an ABB micro-portable greenhouse gas analyzer (MGGA; range: 0.01–100 ppm; precision: < 2 ppb) or Picarro GasScouter (range: 0–20 ppm; precision: < 0.5 ppb) (Phillips et al., 2013; Jackson et al., 2014; Gallagher et al., 2015; Von Fischer et al., 2017; Zimmerle et al., 2017; Weller et al., 2018; Keyes et al., 2020). The height of the sensor mounted on the vehicle varies between 0.3 and 4.5 m depending on the driving survey method, and survey speeds range between 4 and 15 m s^{-1} (9–34 mph) (Phillips et al., 2013; Jackson et al., 2014; Gallagher et al., 2015; Zimmerle et al., 2017; Weller et al., 2018). Even though there is a lot of interest in these survey methods, there is not a clear understanding of best practices, specifically how survey distance, survey height, survey speed, and atmospheric conditions could affect the probability of leak detection. While prior studies have used walking and driving surveys to detect subsurface NG leaks (Phillips et al., 2013; Gallagher et al., 2015; Von Fischer et al., 2017; Weller et al., 2018; Cho et al., 2020; Keyes et al., 2020), the survey detection probability (DP) was not characterized.

Currently, there is no quantitative relationship between subsurface leak rate and DP for controlled belowground leak conditions. Some aboveground emission studies have shown that DP increases with the emission rate (Rella et al., 2015; Ravikumar et al., 2018; Bell et al., 2020). Others suggested that the relationship does not always exist (Ravikumar et al., 2019). One recent study, using a drone with a survey speed of 15–20 m s^{-1} (34–45 mph), showed no relationship between leak rate and DP (Barchyn et al., 2019). Other aboveground studies have found a strong relationship between downwind distance and the DP, where controlled single-blind detection tests using an optical gas imaging (OGI) camera found a power-law relationship between leak size and detection distance between 1.5 and 15 m of the leak source (Ravikumar et al., 2018). Zimmerle et al., 2020 indicated that the experience of OGI surveyors significantly impacted the DP, and highly experienced surveyors detected 1.7 (1.5–1.8) times more aboveground leaks than less experienced surveyors, primarily by adjusting the survey speed.

In addition to leak rate and survey protocols, prior studies have explored how atmospheric conditions, mostly wind speed, affect the DP (Thorpe et al., 2016; Ravikumar et al., 2018; Barchyn et al., 2019; Bell et al., 2020). Similar to the leak rate, the effect of wind speed on DP is unclear. Thorpe et al. (2016) did not find any significant relationship between wind speed and DP using an airborne visible/infrared imaging spectrometer (AVIRIS-NG) during the controlled release experiments. This finding was also consistent with Ravikumar et al. (2018). In contrast, two aboveground controlled release experiments showed that the drone and airplane surveys have the highest DP in moderate wind speeds (2–2.5 m s^{-1}) (Barchyn et al., 2019; Sherwin et al., 2021). A belowground controlled release experiment from Riddick et al. (2021) showed that surface CH_4 mole fractions are mostly affected by atmospheric stability and suggested avoiding walking surveys during strong winds or strong solar irradiance conditions. A recent study (Tian et al., 2022) pointed out that subsurface leaks can be quantified using time-averaged downwind CH_4 concentration measurements. The authors know of no peer-reviewed studies that systematically investigate how leak rate sizes, survey protocols, and atmospheric conditions affect the DP of subsurface NG emissions. Thus, this study aims 1) to investigate how the leak rate, survey distance and speed, and atmospheric conditions affect the DP of a subsurface NG emission; 2) to develop a validated DP model for practitioners that incorporates the leak rate, survey distance, survey speed, and weather conditions including atmospheric stability, wind speed, and air temperature; 3) to model the weighted DP for walking and driving surveys using three published and publicly available emission rate datasets from NG distribution pipeline leaks. To our knowledge, this is the first time that a validated DP model has been developed, considering all critical parameters of the leak survey measured from belowground emission experiments.

2. Material and methods

2.1. Experiment and measurement approaches

Five controlled NG release (87 ± 2 vol % CH4) experiments were conducted from June 21st to July 4th, 2021, with the release rate ranging from 0.5 to 8.5 g min^{-1} (Table 1) at Colorado State University's Methane Emission Technology Evaluation Center (METEC) in Fort Collins, CO, U.S. The release rates were chosen to represent the range of leaks from the underground NG pipelines observed in the field (Lamb et al., 2015; Von Fischer et al., 2017). The testbed used here is a rural testbed with short surface vegetation (average height: 0.05 m). The pipeline was buried at 0.9 m below the ground surface along the east-west direction of the site and backfilled with the native soil (sandy loam, U.S. Department of Agriculture Soil Texture Classification). Gas was injected through stainless-steel tubing (0.635 cm, model SS-T4-S-035-20, Swagelok, USA) into the testbed from an aboveground 145-Liter compressed natural gas (CNG) tank. The gas flow rate was controlled by pressure regulators, solenoid valves, and choked flow orifices. It was measured by a thermal mass flow meter (range: 0–11 g min^{-1}, accuracy: ±1%, Omega FMA1700 series). A detailed description of this testbed can be found in prior publications (Mitton, 2018; Ulrich

Table 1
General information of the five controlled belowground NG release experiments at the METEC site from June 21st to July 4th, 2021. The release rate ranged from 0.5 to 8.5 g min^{-1}. The total number of passing was 3472 for the five experiments.

Exp	Date	Release rate (g min^{-1})	Total number of passings
1	June 21 to June 26, 2021	0.5	1282
2	June 30 to July 01, 2021	0.8	434
3	June 28 to June 29, 2021	1.6	318
4	July 01 to July 02, 2021	3.5	730
5	July 02 to July 04, 2021	8.5	708

et al., 2019; Cho et al., 2020).

During each experiment, CH_4 mole fraction and GPS coordinate data were collected while walking at distances (1, 5, 10, and 20 m) downwind of the emission point and perpendicular to the wind direction. CH_4 mole fractions were measured using a high-precision gas analyzer (GasScouter™ G4301, Picarro, Inc.), with 0.1 ppb measurement precision at a 1 Hz measurement interval. GPS data were collected using a Picarro A0946 unit with a position accuracy of <1 m and 1 Hz update frequency. At each distance downwind of the emission point, transects were measured at three heights (0.05, 0.25, and 0.5 m), which typically simulate both walking and driving surveys (Phillips et al., 2013; Zimmerle et al., 2017; Cho et al., 2020; Riddick et al., 2021). The survey speed was 1 m s^{-1} (~2 mph) on average, and the transect length was 80 m. Here, one complete measurement per distance per height is defined as "one passing", and the total number of passings was 3472 for the five experiments (Table 1). In order to show how survey speed affects detection probability, the measured CH_4 mole fraction data in each walking passing were extended to produce a series of data simulating increased survey speed from 2 to 15 m s-1 (4–34 mph) using a down-sampling method as follows: 1) The walking survey speed is 1 m s-1, and the gas analyzer measures the CH4 mole fraction at 1 Hz. Thus, the walking survey data represent approximately 1 m intervals along the transect in each pass (i.e., 1 m interval in every two adjacent samples); 2) When the survey speed increases to 2 m s-1, every other sample is selected to simulate a 2 m interval in each passing; 3) The down-sampling was repeated for other speeds from 3 to 15 m s-1 by selecting every 3–15 m in each passing, respectively. This approach assumes that the instrument has a fast response time (e.g., 1–10 Hz) and, therefore able to detect the CH4 emissions from the belowground pipeline leaks. Instruments with response times in the 1–10 Hz range are increasingly available in recent years, such as the Li-Cor LI-7700 open path CH4 analyzer (frequency: 10 Hz, precision: < 5 ppb) or the ABB's LGR-ICOS™ ultrasensitive gas analyzer (frequency: 10 Hz; precision < 1 ppb). This down-sampling approach based on a 1–10 Hz frequency instrument may not work well in some situations. For example, if the plume width is less than the sampling interval linked to a fast-driving speed. We also acknowledge that this assumption did not consider the influence of the vehicle on the plume in a real driving survey situation and not always driving downwind of the emission source. The 3D wind fields, and air temperature were measured at 8 Hz using an RM Young 81000 Ultrasonic Anemometer installed 6 m above the ground at the METEC site. Previous studies (Bosveld and Beljaars, 2001; Bardal et al., 2018) have shown that the 3D sonic anemometer measurements with varying sampling intervals between 1 and 10 Hz do not influence the average vertical flux estimate. However, the uncertainty in the flux estimate increases with a decrease in the sampling interval. Therefore, the 8 Hz sampling interval used in this study will generally satisfy sampling rate requirements to estimate the average vertical flux and stability parameter (i.e., Monin-Obukhov length) accurately.

2.2. Methodology

In this work, the subsurface leak was defined as either detection or non-detection for each pass along the pipeline. A pass was considered a detection if a 0.2 ppm CH_4 mole fraction enhancement was observed over the 2.0 ppm background (10% change) at the METEC site. The background CH_4 mole fraction was calculated by averaging the measurements 10 m upwind of the subsurface leaks. This threshold is consistent with a previous study that used the driving survey to conduct pipeline leak detection in 15 metro areas (Luetschwager et al., 2021). The empirical DP was calculated as the number of detected passes divided by the total number of passes.

The 5-min averaged Monin-Obukhov length (L, m) was calculated (Equations (1) and (2); Flesch et al., 2004; Foken, 2006; Stull, 2012) from the surface friction velocity (u*, m s^{-1}), the mean absolute air temperature (T, K), the von Kármán's constant (k_v = 0.41), the gravitational acceleration (g = 9.81 m s^{-2}), and 3D horizontal/vertical wind vectors (u, v, and w, m s^{-1}). In accordance with previous studies, the sonic temperature, approximately equal to virtual temperature, was used for T in calculating L (Flesch et al., 2004; Foken, 2006). Any resulting error in L from using sonic temperature rather than virtual temperature should be small as the experiments were conducted in dry air conditions (relative humidity: approx. 30%) (Flesch et al., 2004). The Monin-Obukhov length was also converted into Pasquill-Gifford (PG) stability class as it is more quickly recognized than L by industry practitioners (Ulrich et al., 2019; Riddick et al., 2021) where PG A (extremely unstable) is $-100 \le L < 0$, PG B/C (unstable) is $-500 \le L < -100$, PG D (neutral) is $|L| > 500$, PG E/F (stable) is $500 \le L < 100$, and PG G (extremely stable) is $0 < L \le 100$ (Gryning et al., 2007; Breedt et al., 2018).

$$L = -\frac{u_*^3 T}{k_v g \overline{w'T'}} \tag{1}$$

$$u_* = \left[\left(\overline{u'w'}\right)^2 + \left(\overline{v'w'}\right)^2\right]^{1/4} \tag{2}$$

The empirical DP data were randomly split into two parts, i.e., 80% as training data for developing the DP model, and 20% as test data for validating the DP model. The DP model was developed by fitting the training data with a multiple logistic function (Equation (3)), which is similar to previous studies that used a single logistic function to fit the empirical DP and leak rate (Ravikumar et al., 2018; Luetschwager et al., 2021). The variables considered in the DP model include the leak rate, survey distance, survey speed, atmospheric stability (1/L), wind speed, and air temperature. A p-value of less than 0.05 was used to ensure the variables considered in the model are at least 95% statistically significant. The coefficient of determination (R^2) was used as a metric to validate the performance of the DP model by comparing modeled DP with the empirical DP from test data.

$$DP = \frac{1}{1 + e^{-\left(b_0 + b_1 q + b_2 c + b_3 s + \frac{b_4}{L} + b_5 U + b_6 T\right)}} \tag{3}$$

where b_0 is the intercept, $b_1, .., b_6$ are the regression coefficients, q is the leak rate (g min^{-1}), c is the survey speed (mph), s is the survey distance (m), L is the Monin-Obukhov length (m), U is the horizontal wind speed (m s^{-1}), and T is the air temperature (°C).

Using the validated DP model and three publicly available NG pipeline emission datasets (Table 2), we modeled the weighted DP (Equation (4)) to quantity detection efficiency of walking and driving survey (Table 3) in a range of atmospheric stability and wind speed conditions. The emission datasets (Table 2) were directly measured by the surface chamber from NG distribution main and service line leaks across U.S. (Lamb et al., 2015; Hendrick et al., 2016; GTI, 2019). The total sample size is 446, characterized by a right-skewed distribution. Three super large emitters (16, 24, and 38 g min^{-1}) were removed to be consistent with the range of the controlled leak rates. Thus, there are 443

Table 2
General information of three publicly available CH_4 emission rate datasets from NG distribution pipelines. Emission rates in these three datasets were measured directly using surface flux chambers, where all datasets show a right-skewed distribution characteristic. The total sample size used is 443. Three super large emission points were removed to be consistent with the range of controlled NG release rates in the DP model.

Location	Sample size	Leak source	Reference
California	76	NG distribution mains and services	GTI (2019)
Massachusetts	113	NG distribution mains	Hendrick et al. (2016)
U.S. (various)	257	NG distribution mains and services	Lamb et al. (2015)

Table 3
Survey distance and speed for walking and driving surveys. The assumed driving survey speed is 11, 22, and 34 mph, which represents the low, medium, and high speeds of the field driving survey, respectively. The survey distance was assumed as 5 m downwind of the pipeline based on general field survey practices.

Survey solution	Survey distance (m)	Survey speed (mph)
Walking survey	5	2
Driving survey	5	11
Driving survey	5	22
Driving survey	5	34

emission rate points used in the DP model. The survey distance was assumed as 5 m downwind of the pipeline, based on general practice during the field pipeline survey. The driving survey speed was assumed as 11, 22, and 34 mph. These speeds are based on low, medium, and high speeds seen in previous field studies of driving surveys (Phillips et al., 2013; Jackson et al., 2014; Gallagher et al., 2015; Zimmerle et al., 2017; Weller et al., 2018).

$$f = \frac{\sum_{i=1}^{n} DP_i q_i}{\sum_{i=1}^{n} q_i} \quad (4)$$

where f is the weighted DP, DP_i is the modeled DP for the ith emission rate q_i (unit: g min^{-1}), n is the total number of emission points (n = 443).

3. Results

3.1. Empirical detection probability with different survey speeds

Fig. 1 showed the empirical DP as a function of distance with the mobile survey speed ranging from 2 to 34 mph from the five controlled experiments (Table 1). The result showed that the empirical DP decreases with the increase in survey speed. The empirical DP increases with the leak rate near the emission point (<5 m). The empirical DP is between 70% and 100% at a 1 m distance for an emission rate between 0.5 and 8.5 g min^{-1} at a low survey speed (between 2 and 11 mph). DP decreases with the increase in survey distance, especially for the smallest leak (0.5 g min^{-1}), where the detection probability is 25% at a 20 m distance from the leak source (Fig. 1a). For the medium to large leak (0.8–8.5 g min^{-1}), the detection probability decreases to between 50% and 80% at a 20 m downwind distance at a low survey speed (2–11 mph). When the survey speed increases (medium survey speed between 11 and 22 mph), the empirical DP is between 25% and 75% at a 1 m downwind distance, and mostly between 25% and 50% at a 20 m distance. Further, the empirical DP is less than 25% at any distance regardless of leak size when the survey speed is high (22–34 mph). Besides, compared to Exp1-4, the DP in Exp5 mostly showed an increase with the increase in survey distance considered here for a given survey speed. This is probably due to the largest leak rate (8.5 g min^{-1}) in Exp5, which is large enough to produce a broader plume at a farther downwind distance than that at a closer downwind distance to the subsurface leak source. Thus, for a given survey speed, it is more likely to grab a sample within the broader plume at a farther downwind distance than that at a closer distance when the leak rate is large enough (e.g., >8.5 g min^{-1}).

3.2. Empirical detection probability with different atmospheric stability conditions

In general, the empirical DP decreases as the atmospheric stability become more stable (PG: A to G) regardless of the survey speed (Fig. 2). The DP in PG A is between 75% and 100% for the leak rates between 0.5 and 8.5 g min^{-1} with a low survey speed (2–11 mph). With the same low survey speed, the DP decreases to between 45% and 90%, 40% and 85%, 50% and 80%, and 30% and 90% in PG B/C, D, E/F, and G, respectively. When the survey speed increases (medium survey speed between 11 and 22 mph), the empirical DP in PG A is between 50% and 80% for the leak rates considered here. The DP further reduces to between 25% and 75%, 20% and 70%, 25% and 75%, and 15% and 70% in PG B/C, D, E/F, and G, respectively. When the survey speed increases to high (22–34 mph), the empirical DP is generally less than 25% in PG A, B/C, D, E/F, and G, respectively, for the range of emission rates considered here.

Generally, each PG stability class can be roughly estimated based on a range of wind speeds (Pasquill, 1961). Calm (0–1 m s^{-1}), small (1–3 m s^{-1}), and medium winds (3–5 m s^{-1}) typically occur during unstable or stable conditions (PG A, B/C, E/F, G). Medium and large winds (5–10 m s^{-1}) generally occur during neutral conditions (PG D). Fig. 3 further shows the relationship between the empirical DP and the binned wind speed for mobile survey speeds ranging from 2 to 34 mph for the five controlled experiments (Exp1–5). The empirical DP generally decreases with an increase in wind speed. For low survey speeds (2–11 mph), the DP is highest in calm wind conditions (0–1 m s^{-1}), ranging from 70% to 100%. With the same low survey speed, the DP is generally the lowest in large wind conditions (5–10 m s^{-1}), ranging from 30% to 90%. When the survey speed increases to between 11 and 22 mph (medium speeds), the empirical DP reduces to between 25% and 75%. When the survey speed increases to high speeds (22–34 mph), the empirical DP is generally less than 25%, regardless of wind conditions.

3.3. Validation of the detection probability model

All variables considered here are at least 95% statistically significant, with p values less than 0.05 (Table 4). The height variable did not pass the 95% statistically significant test and was therefore removed from the DP model. This is probably due to the small change in plume width for the height range considered in this study (0.05–0.5 m), thereby not

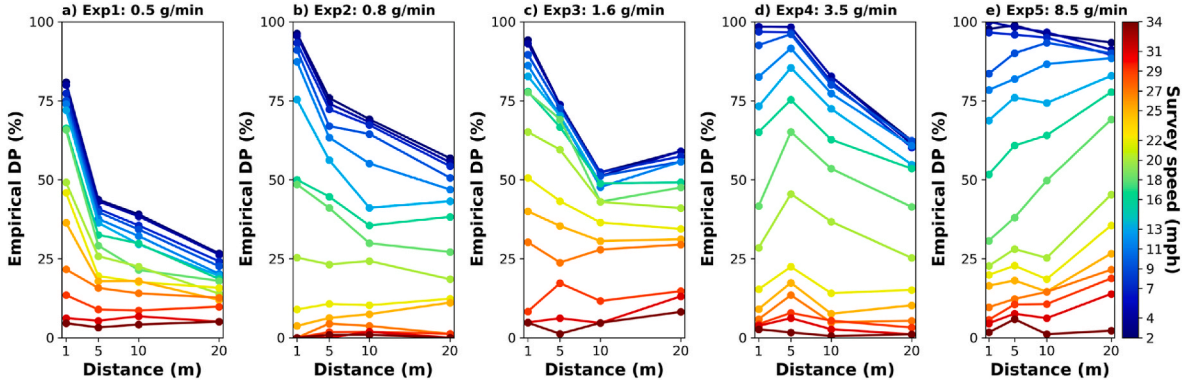

Fig. 1. Empirical detection probability as a function of distance with the mobile survey speed ranging from 2 to 34 mph for the five controlled experiments (Exp1–5), respectively.

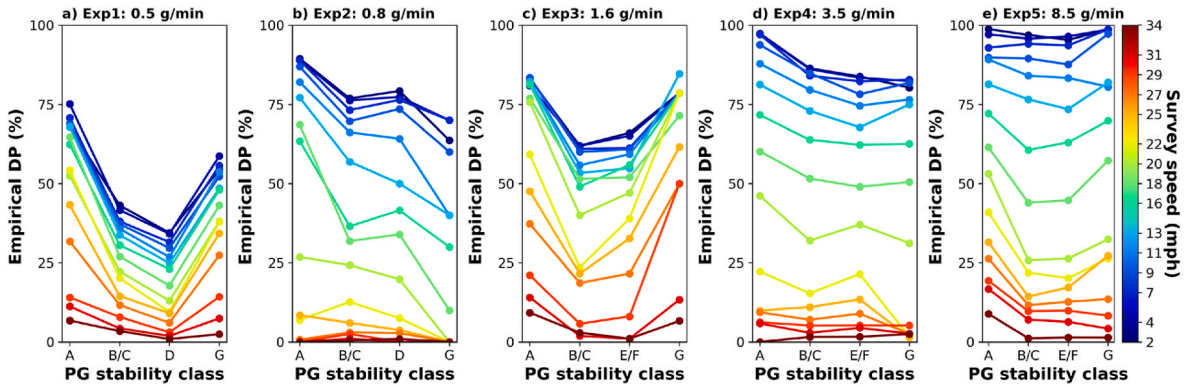

Fig. 2. Empirical detection probability as a function of the Pasquill-Gifford (PG) stability class with the mobile survey speed of 2–34 mph for the five controlled experiments (Exp1–5), respectively. PG stability class A denotes the extremely unstable condition, PG stability class B/C denotes the unstable condition, PG stability class D denotes the neutral condition, PG stability class E/F denotes the stable condition, and PG stability class G denotes the extremely stable condition. No observation data is available for PG stability class E/F in Exp1–2, and PG stability class D for Exp 3–5.

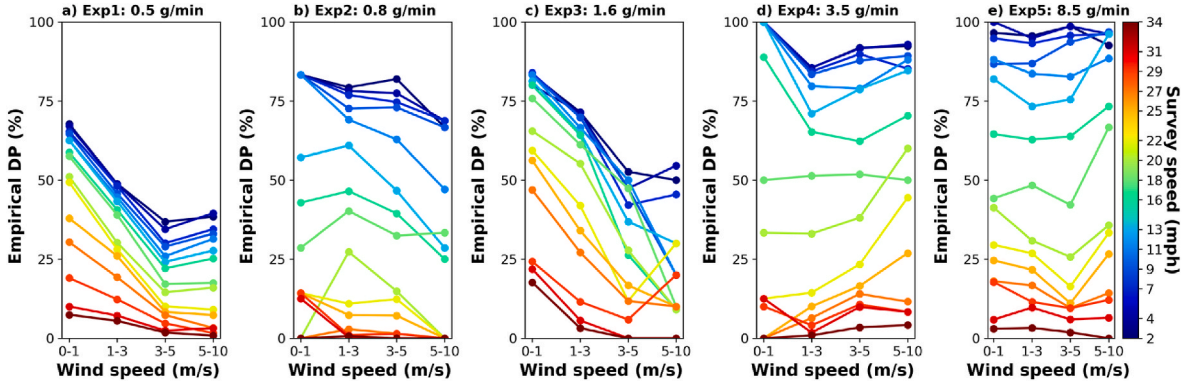

Fig. 3. Empirical detection probability as a function of the binned wind speed with the mobile survey speed of 2–34 mph for the five controlled experiments (Exp1–5), respectively. The binned wind speed interval is 0–1, 1–3, 3–5, and 5–10 m s^{-1}, representing the calm, low, medium, and large wind conditions, respectively, according to the measured wind speed range during the experiments.

Table 4
Estimated mean regression coefficients and the respective p values in the fitted model. μ is the mean value, σ is the standard error (SE). μ and σ were calculated by bootstrapping the training data 1000 times.

$$DP = \frac{1}{1 + e^{-\left(5.0221 + 0.139q - 0.1498c - 0.057s - \frac{12.7024}{L} - -0.4115U - 0.0807T\right)}} \quad (5)$$

Parameter	Regression coefficient ($\mu \pm 1\ \sigma$)	p value ($\mu \pm 1\ \sigma$)
Intercept (b_o)	5.0221 ± 0.0117	6.14761E-39 ± 3.65743E-39
Leak rate (b_1)	0.139 ± 0.0005	4.7734E-16 ±4.34151E-16
Survey speed (b_2)	−0.1498 ± 0.0002	1.0119E-102 ± 9.1455E-103
Survey distance (b_3)	−0.057 ± 0.0002	1.26593E-13 ± 1.3302E-13
Monin-Obukhov length (b_4)	−12.7024 ± 0.0976	1.0586E-04 ± 4.99716E-05
Wind speed (b_5)	−0.4115 ± 0.0021	1.5131E-07 ± 5.2156E-08
Air temperature (b_6)	−0.0807 ± 0.0006	4.279E-06 ± 2.45119E-06

having a significant effect on DP. The leak rate is positively related to the DP with the regression coefficient of 0.139 ± 0.0005 (Table 4). The regression coefficients for survey speed, survey distance, Monin-Obukhov length, wind speed, and air temperature are all negative, with the largest ones from the Monin-Obukhov length, wind speed, and survey speed, respectively. The regression coefficients from air temperature and survey distance are relatively low, with the values of −0.0807 ± 0.0006, and −0.057 ± 0.0002. Using the regression coefficients in Table 4, the DP model was rewritten as a function of the leak rate, survey distance, survey speed, Monin-Obukhov length, wind speed, and air temperature (Equation (5)). When compared with the empirical DP from the test data, the model shows good performance, with a coefficient of determination (R^2) of 0.76 (Fig. 4).

The sensitivity analysis of variables in the DP model showed that survey speed, atmospheric stability (1/L), and wind speed take the most significant effects on the DP (Fig. 5). DP reduces 20%–30% when changing survey speed from 2 to 34 mph, atmospheric stability (1/L) from −0.2 to 0.2 m^{-1}, and wind speed from 1 to 10 m s^{-1}, respectively. The change in DP is less than 5% when changing leak rate from 0.5 to 8.5 g min^{-1}, survey distance from 1 to 20 m, and air temperature from 15 to 30 °C, respectively. The increase in modeled DP from the sensitivity analysis with an increase in leak rate is smaller than the increase in the empirical DP shown previously (e.g., Fig. 1a and e). This is because the empirical DP includes the impacts of other factors such as atmospheric stability and wind speed. Overall, the modeled DP still reveals the increased trend of DP with the leak rate, which is consistent with observations.

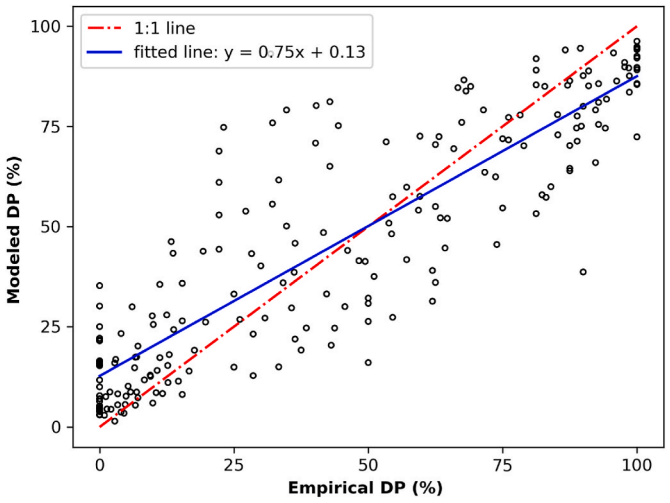

Fig. 4. Modeled DP vs Empirical DP. The empirical DP is from the test data. The red dashed line is the 1:1 line. The blue line is the fitted equation between Modeled DP and Empirical DP where y is Modeled DP, and x is Empirical DP. The coefficient of determination (R^2) between Modeled DP and Empirical DP is 0.76. (For interpretation of the references to colour in this figure legend, the reader is referred to the Web version of this article.)

3.4. Modeled detection probability for walking and driving surveys

Given the right-skewed distribution of emissions from the pipeline leaks (Lamb et al., 2015; Hendrick et al., 2016; GTI, 2019), here we modeled the DP for the small and large leaks across different survey speeds, atmospheric stabilities, and wind speed conditions (Fig. 6). Modeled DP is higher than 90% under the conditions of PG stability class A, low survey speed (2–11 mph), and calm to medium wind speed (0–5 m s^{-1}), regardless of leak rate. However, when the PG stability class changes to G, modeled DP is less than 50%, and 70% for the small and large leak, respectively, under such a low survey speed and wind speed condition. Modeled average DP reduces about 5%–25% with the increase in wind speed and survey speed, regardless of PG stability class and leak rate. Generally, as the atmosphere changes from PG stability class A to G, the CH_4 plume becomes more narrow and concentrated, due to the decrease in the gas dispersion (Riddle et al., 2004; Leelőssy et al., 2014; Tian et al., 2022). Also, wind speed has been shown to influence the plume shape and size (Carpenter et al., 1971; Thorpe et al., 2016). During high wind speed conditions, the plume has a longer length and narrower width, but it is shorter and wider during low wind conditions (Thorpe et al., 2016). Thus, it is expected that DP is higher in a wider plume than in a narrower plume for each downwind transect survey along the pipeline because one is more likely to collect at least one sample within the plume. That is, for a certain plume width and fixed sample frequency, a higher survey speed results in coarse CH_4 sampling points during each transect, therefore DP is lower in high survey speed than in low survey speed.

Further, using the publicly available subsurface emission rates measured across the U.S., we modeled the weighed DP to inform the overall detection efficiency of walking and driving surveys on a national scale (Fig. 7). The weighted average DP in all PG stability class conditions is 83% on average for the walking survey at a calm wind speed (0–1 m s^{-1}). But it reduces to 67%, 42%, and 19% for the driving survey with a low, medium, and high survey speed, respectively. For a high wind speed that typically occurs in PG D (5–10 m s^{-1}), the weighted average DP is less than 37% for all surveys considered here. With the increase of survey speed, the options of favorable weather conditions (i.e., PG stability class and wind speed) are rapidly decreased for having a high DP. For example, the walking survey has a DP higher than 50% in the PG stability class ranging from A to E/F and calm to medium wind speed conditions (0–5 m s^{-1}). However, this can only be achieved at a calm to low wind speed (0–3 m s^{-1}) for a driving survey at a low speed of 11 mph. When the driving survey speed increases to 34 mph, there is only calm wind in PG A favorable for a DP higher than 50%.

Our results show that DP highly depends on survey speed, atmospheric stability, and wind speed. A higher DP tends to be achieved when surveying at a lower survey speed, atmospheric stability (1/L), and wind speed conditions. The average DP in all weather conditions (PG A to G, calm to large winds) is about 66% for the walking survey, which is close to the assumed 85% detection probability for quantifying the CH_4 emissions from the U.S. NG distribution pipelines (Campbell et al., 1996; Lamb et al., 2015). For a driving survey with low to medium speed (11–22 mph), the average DP in all weather conditions is about

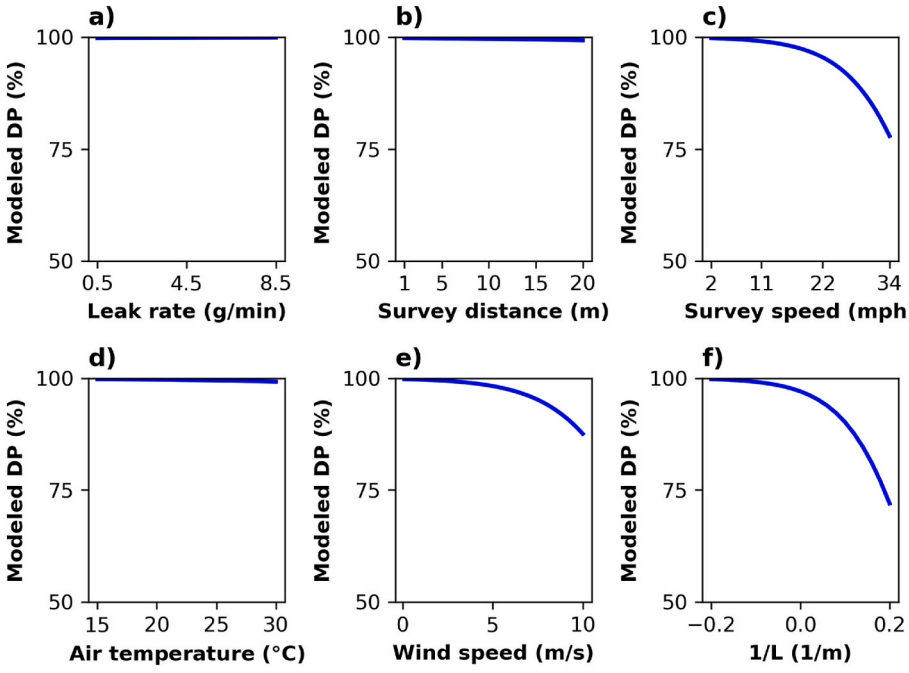

Fig. 5. Sensitivity analysis of each variable in the model on modeled DP. a)–f) shows the effect of changing leak rate, survey distance, survey speed, air temperature, wind speed, and 1/L input, respectively, while keeping other variables the same as the base case. In the base case, the leak rate is 0.5 g min^{-1}, survey speed is 2 mph, survey distance is 1 m, air temperature is 15 °C, wind speed is 0.1 m s^{-1}, and 1/L is −0.2 m^{-1}. The value of each variable in the base case is the lower limit of the data used for developing the DP model. The maximum value of each variable in a)–f) is the upper limit of the data used for developing the DP model.

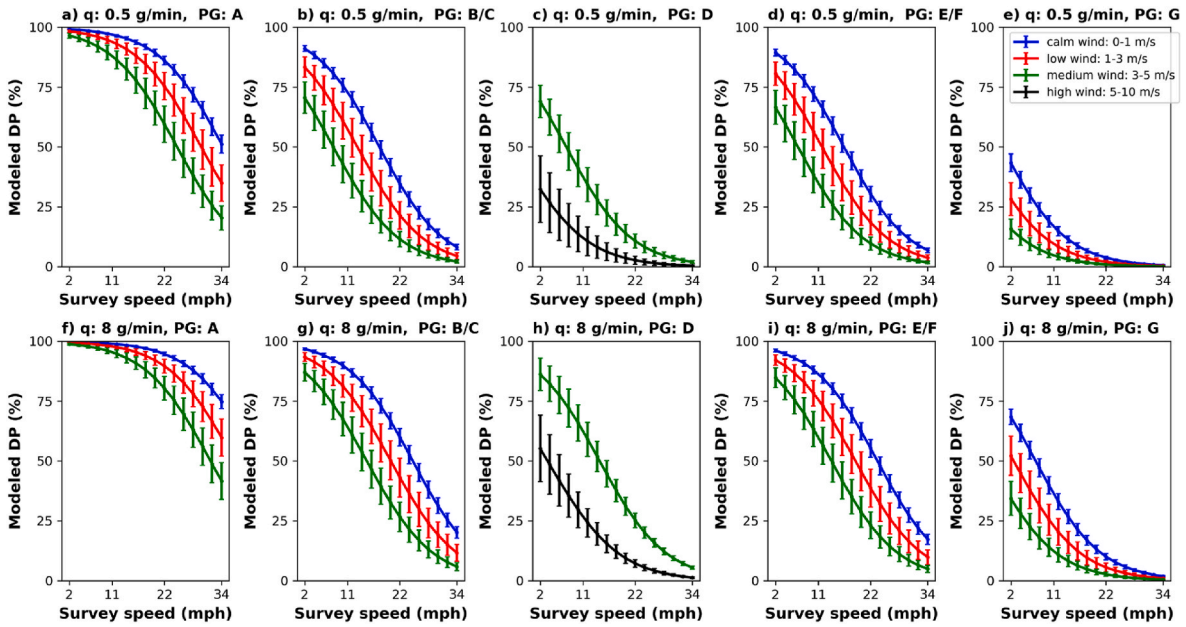

Fig. 6. Modeled DP as a function of survey speed under different PG stability classes and wind speed conditions. a)–e) is the modeled DP for a small leak (q: 0.5 g min^{-1}). f)–j) is the modeled DP for a large leak (q: 8 g min^{-1}). The survey distance is 5 m, air temperature is 25 °C (average temperature during the experiments). The calm wind is 0–1 m s^{-1}, the low wind is 1–3 m s^{-1}, the medium wind is 3–5 m s^{-1}, and the high wind is 5–10 m s^{-1} according to the measured wind speed range during the experiments. The value of 1/L is −0.2, −0.05, 0.001, 0.05 and 0.2 m^{-1} for PG stability class A, B/C, D, E/F and G, respectively. The error bar is ±1 standard deviation. Note, calm, small, and medium winds typically occur during unstable or stable conditions (PG A, B/C, E/F, G). Medium and large winds generally occur during neutral conditions (PG D) (Pasquill, 1961).

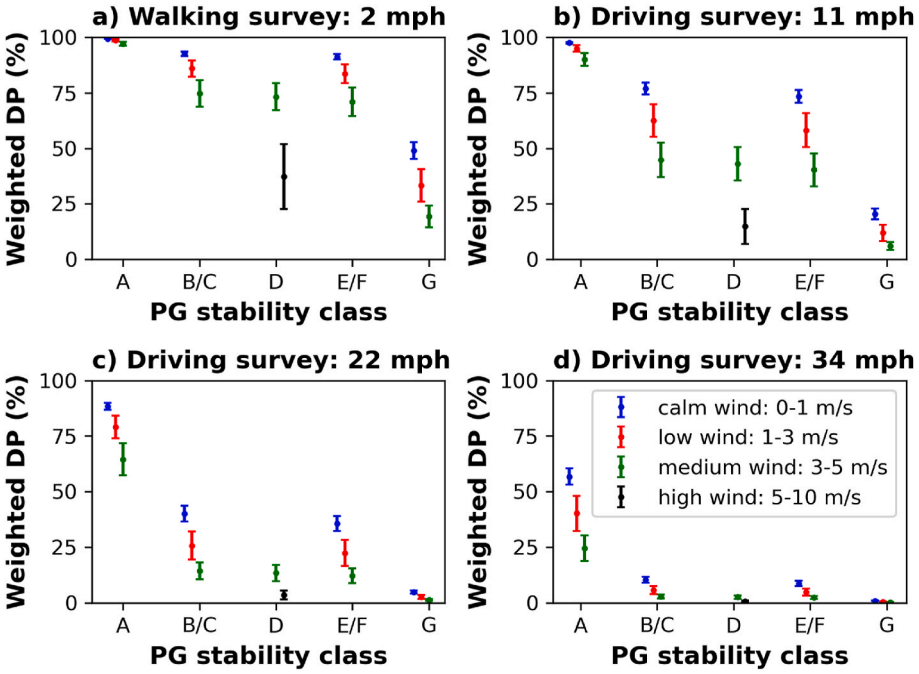

Fig. 7. Weighed DP for walking and driving surveys under different PG stability and wind speed conditions. The survey distance is 5 m, air temperature is 25 °C (average temperature during the experiments). The emission rate is from three publicly available emission rate datasets (Table 2). The calm wind is 0–1 m s^{-1}, the low wind is 1–3 m s^{-1}, the medium wind is 3–5 m s^{-1}, and the high wind is 5–10 m s^{-1} according to the measured wind speed range during the experiments. The value of 1/L is −0.2, −0.05, 0.001, 0.05 and 0.2 m^{-1} for PG stability class A, B/C, D, E/F and G, respectively. The assumed driving survey speeds are 11 and 22, 34 mph, representing the field survey's low, medium, and high driving speeds, respectively (Table 3). The error bar is ±1 standard deviation. Note, calm, small, and medium winds typically occur during unstable or stable conditions (PG A, B/C, E/F, G). Medium and large winds generally occur during neutral conditions (PG D) (Pasquill, 1961).

35%, with the highest DP (>80%) under PG A and calm to low wind conditions (0–3 m s^{-1}). Similar to this survey speed range, the field campaign from Weller et al. (2018) showed that their mobile survey method could detect 75% of pipeline leaks, but only 35% were successfully located by local distribution company field crews. As no weather information was provided, it is unknown if their mobile surveys corresponded with the weather conditions tested in this study. Overall, the walking survey has a wide range of favorable weather conditions ranging from PG stability class A to E/F and calm to medium winds (0–5 m s^{-1}) to get a high DP (e.g., at least 50% likely to detect a leak when one is present). The driving survey has limited favorable weather conditions to achieve an equivalent DP. A driving survey with a low speed (11 mph) should survey under the calm to low wind speed (0–3 m s^{-1}) and PG stability class A to E/F conditions to have an equivalent DP to a walking survey. When the survey speed increases to a medium speed (22 mph), the optimum weather condition is limited to the PG stability class A and calm to medium wind speed conditions (0–3 m s^{-1}). Only calm wind conditions in PG A (0–1 m s^{-1}) are favorable to get an equivalent

DP at a high driving survey speed (34 mph).

4. Conclusions

4.1. Leak detection

This work characterizes the probability of mobile survey solutions to detect underground pipeline leaks using a comprehensive approach. Our results showed that the empirical DP decreases with the increase in survey speed, survey distance, atmospheric stability (1/L), wind speed, and air temperature, but is positively proportional to the leak rate. Survey speed, atmospheric stability, and wind speed significantly impact the DP. For subsurface leak rates (0.5–8.5 g min^{-1}) considered here, the average empirical DP in PG A is 85% at a low survey speed (2–11 mph) and 68%, 63%, 65%, and 60% in PG B/C, D, E/F, and G respectively. As the survey speed increases to 22–34 mph, the average DP is generally less than 25%, regardless of PG stability class conditions and leak rates considered here. The sensitivity analysis showed that the average modeled DP has a decrease of 25% with an increase in survey speed from 2 to 34 mph, atmospheric stability (1/L) from −0.2 to 0.2 m^{-1}, and wind speed from 0.1 to 10 m s^{-1}, respectively.

The findings of this study emphasize the importance of the leak rate, survey protocols (i.e., survey distance, and speed), and weather conditions (i.e., atmospheric stability, wind speed, air temperature) in influencing the detection efficiency of leak survey solutions. Our work presents a validated DP model for driving survey solution providers to optimize survey conditions to have an equivalent DP to the traditional walking survey.

4.2. Implications for leak detection solutions

The driving survey has been increasingly used to detect and/or assess the NG pipeline leaks (Von Fischer et al., 2017; Zimmerle et al., 2017; Li et al., 2020; Weller et al., 2020; Defratyka et al., 2021). The primary advantage of the driving survey is that one can cover more areas more rapidly than a walking survey. However, there is no robust evidence proving that a driving survey is at least as effective in detecting subsurface leaks as the traditional waking survey. Thus, gaps remain in our understanding of the effectiveness of driving survey efforts in detecting subsurface leaks.

This study analyzed the DP of walking and driving surveys in a comprehensive fashion using data from both a newly developed subsurface leak data set and previous studies available in the literature. Our results showed that with the increase of survey speed, the options of favorable weather conditions (i.e., PG stability class and wind speed) rapidly decrease when trying to achieve a high DP (e.g., >50%). The walking survey has a wider range of weather conditions for high DP, ranging from PG stability class A to E/F and clam to medium winds (0–5 m s^{-1}). The driving survey with a low survey speed of 11 mph can only be conducted under calm to low wind speed conditions (0–3 m s^{-1}) to have an equivalent DP to a walking survey. When driving survey speed increases to 34 mph, only calm wind conditions in PG A (0–1 m s^{-1}) are favorable to get an equivalent DP. The driving survey solution providers need to choose a suitable survey speed under different weather conditions to achieve a DP equivalence to the traditional walking survey.

Author contributions

Shanru Tian: Conceptualization, Data curation, Methodology, Formal analysis, Investigation, Writing Original Draft, Review, and Editing. Stuart N. Riddick: Conceptualization, Methodology, Review, Editing, Project Administration, and Funding Acquisition. Younki Cho: Conceptualization, Data curation, Methodology, Review, Editing. Clay S. Bell: Conceptualization, Methodology, Review, and Editing. Daniel J. Zimmerle: Conceptualization, Methodology, Review, Editing, Project Administration, Funding Acquisition. Kathleen M. Smits: Conceptualization, Methodology, Review, Editing, Supervision, Funding acquisition, Project administration.

Declaration of competing interest

The authors declare that they have no known competing financial interests or personal relationships that could have appeared to influence the work reported in this paper.

Data availability

Data will be made available on request.

Acknowledgments

This research was jointly funded by the Colorado Oil and Gas Conservation Commission (COGCC) Mark Martinez & Joey Irwin Memorial Public Projects Fund and the US Department of Transportation (DOT) Pipeline and Hazardous Materials Safety Administration (PHMSA) under Grant No. 693JK32010011POTA. The authors would also like to acknowledge Aidan Duggan for the technical assistance. Any opinion, findings, conclusions, or recommendations expressed herein are those of the authors and do not necessarily reflect the views of those providing technical input or financial support. The trade names mentioned herein are merely for identification purposes and do not constitute an endorsement by any entity involved in this study.

References

Alvarez, R.A., Pacala, S.W., Winebrake, J.J., Chameides, W.L., Hamburg, S.P., 2012. Greater focus needed on methane leakage from natural gas infrastructure. Proc. Natl. Acad. Sci. U. S. A. 109 (17), 6435–6440. https://doi.org/10.1073/pnas.1202407109.

Barchyn, T.E., Hugenholtz, C.H., Fox, T.A., 2019. Plume detection modeling of a drone-based natural gas leak detection system. Elem Sci Anthr 7. https://doi.org/10.1525/elementa.379.

Bardal, L.M., Onstad, A.E., Sætran, L.R., Lund, J.A., 2018. Evaluation of methods for estimating atmospheric stability at two coastal sites. Wind Eng. 42 (6), 561–575. https://doi.org/10.1177/0309524X18780378.

Bell, C.S., Vaughn, T., Zimmerle, D., 2020. Evaluation of next generation emission measurement technologies under repeatable test protocols. Elem Sci Anthr 8. https://doi.org/10.1525/elementa.426.

Bosveld, F.C., Beljaars, A.C.M., 2001. The impact of sampling rate on eddy-covariance flux estimates. Agric. For. Meteorol. 109 (1), 39–45. https://doi.org/10.1016/S0168-1923(01)00257-X.

Breedt, H.J., Craig, K.J., Jothiprakasam, V.D., 2018. Monin-Obukhov similarity theory and its application to wind flow modelling over complex terrain. J. Wind Eng. Ind. Aerod. 182, 308–321. https://doi.org/10.1016/j.jweia.2018.09.026.

Campbell, L.M., Campbell, M.V., Epperson, D., 1996. Methane Emissions from the Natural Gas Industry Volume 9: Underground Pipelines. U.S. Environmental Protection Agency, Washington, D.C. EPA/600/R-96/080i (NTIS PB97-143002). Available at: Accessed 5 Feb 2022.

Carpenter, S.B., Montgomery, T.L., Leavitt, J.M., Colbaugh, W.C., Thomas, F.W., 1971. Principal plume dispersion models: TVA power plants. J. Air Pollut. Control Assoc. 21 (8), 491–495. https://doi.org/10.1080/00022470.1971.10469560.

Cho, Y., Ulrich, B.A., Zimmerle, D.J., Smits, K.M., 2020. Estimating natural gas emissions from underground pipelines using surface concentration measurements. Environ. Pollut. 267, 115514 https://doi.org/10.1016/j.envpol.2020.115514.

Defratyka, S.M., Paris, J.D., Yver-Kwok, C., Fernandez, J.M., Korben, P., Bousquet, P., 2021. Mapping urban methane sources in Paris, France. Environ. Sci. Technol. 55 (13), 8583–8591. https://doi.org/10.1021/acs.est.1c00859.

Von Fischer, J.C., Cooley, D., Chamberlain, S., Gaylord, A., Griebenow, C.J., Hamburg, S. P., Salo, J., Schumacher, R., Theobald, D., Ham, J., 2017. Rapid, vehicle-based identification of location and magnitude of urban natural gas pipeline leaks. Environ. Sci. Technol. 51 (7), 4091–4099. https://doi.org/10.1021/acs.est.6b06095.

Flesch, T.K., Wilson, J.D., Harper, L.A., Crenna, B.P., Sharpe, R.R., 2004. Deducing ground-to-air emissions from observed trace gas concentrations: a field trial. J. Appl. Meteorol. 43 (3), 487–502. https://doi.org/10.1175/1520-0450(2004)043<0487:DGEFOT>2.0.CO.

Foken, T., 2006. 50 years of the Monin-Obukhov similarity theory. Boundary-Layer Meteorol. 119 (3), 431–447. https://doi.org/10.1007/s10546-006-9048-6.

Gallagher, M.E., Down, A., Ackley, R.C., Zhao, K., Phillips, N., Jackson, R.B., 2015. Natural gas pipeline replacement programs reduce methane leaks and improve consumer safety. Environ. Sci. Technol. Lett. 2 (10), 286–291. https://doi.org/10.1021/acs.estlett.5b00213.

Gryning, S.E., Batchvarova, E., Brümmer, B., Jørgensen, H., Larsen, S., 2007. On the extension of the wind profile over homogeneous terrain beyond the surface

boundary layer. Boundary-Layer Meteorol. 124 (2), 251–268. https://doi.org/10.1007/s10546-007-9166-9.
GTI, 2019. Quantifying Methane Emissions from Distribution Pipelines in California. Available at: Accessed 29 May 2022.
Heath Consultants, 2009. RMLD user's mannual. Available at: Accessed 23 Apr 2022.
Heath, G., Warner, E., Warner, E., Brandt, A., 2015. Estimating U.S. Methane Emissions from the Natural Gas Supply Chain: Approaches, Uncertainties, Current Estimates, and Future Studies. National Renewable Energy Lab.(NREL), Golden, CO (United States). https://doi.org/10.2172/1226158. No. NREL/TP-6A50-62820).
Hendrick, M.F., Ackley, R., Sanaie-Movahed, B., Tang, X., Phillips, N.G., 2016. Fugitive methane emissions from leak-prone natural gas distribution infrastructure in urban environments. Environ. Pollut. 213, 710–716. https://doi.org/10.1016/j.envpol.2016.01.094. Elsevier Ltd.
IPCC, 2014. Anthropogenic and natural radiative forcing. In: Climate Change 2013 – the Physical Science Basis: Working Group I Contribution to the Fifth Assessment Report of the Intergovernmental Panel on Climate Change. Cambridge University Press, Cambridge UK, pp. 659–740. https://doi.org/10.1017/CBO9781107415324.018.
Jackson, R.B., Down, A., Phillips, N.G., Ackley, R.C., Cook, C.W., Plata, D.L., Zhao, K., 2014. Natural gas pipeline leaks across Washington, DC. Environ. Sci. Technol. 48 (3), 2051–2058. https://doi.org/10.1021/es404474x.
Keyes, T., Ridge, G., Klein, M., Phillips, N., Ackley, R., Yang, Y., 2020. An enhanced procedure for urban mobile methane leak detection. Heliyon 6 (10), e04876. https://doi.org/10.1016/j.heliyon.2020.e04876. Elsevier Ltd.
Lamb, B.K., Edburg, S.L., Ferrara, T.W., Howard, T., Harrison, M.R., Kolb, C.E., Townsend-Small, A., Dyck, W., Possolo, A., Whetstone, J.R., 2015. Direct measurements show decreasing methane emissions from natural gas local distribution systems in the United States. Environ. Sci. Technol. 49 (8), 5161–5169. https://doi.org/10.1021/es505116p.
Leelőssy, Á., Molnár, F., Izsák, F., Havasi, Á., Lagzi, I., Mészáros, R., 2014. Dispersion modeling of air pollutants in the atmosphere: a review. Cent. Eur. J. Geosci. 6 (3), 257–278. https://doi.org/10.2478/s13533-012-0188-6.
Levi, M., 2013. Climate consequences of natural gas as a bridge fuel. Clim. Change 118 (3), 609–623. https://doi.org/10.1007/s10584-012-0658-3.
Li, H.Z., Mundia-Howe, M., Reeder, M.D., Pekney, N.J., 2020. Gathering pipeline methane emissions in utica shale using an unmanned aerial vehicle and ground-based mobile sampling. Atmos 11 (7), 1–13. https://doi.org/10.3390/atmos11070716.
Luetschwager, E., von Fischer, J.C., Weller, Z.D., 2021. Characterizing detection probabilities of advanced mobile leak surveys: implications for sampling effort and leak size estimation in natural gas distribution systems. Elementa 9 (1), 1–13. https://doi.org/10.1525/elementa.2020.00143.
Mitton, M., 2018. Subsurface Methane Migration from Natural Gas Distribution [M.S. Thesis]. Colorado School of Mines, Dept. of Civil and Environmental Engineering, Golden, CO. Available at: Accessed 2 May 2022.
National Academies of Sciences, EM, 2022. Nat. Gas. Available at: Accessed 14 May 2022.
Nisbet, E.G., Fisher, R.E., Lowry, D., France, J.L., Allen, G., Bakkaloglu, S., Broderick, T. J., Cain, M., Coleman, M., Fernandez, J., Forster, G., Griffiths, P.T., Iverach, C.P., Kelly, B.F.J., Manning, M.R., Nisbet-Jones, P.B.R., Pyle, J.A., Townsend-Small, A., al-Shalaan, A., et al., 2020. Methane mitigation: methods to reduce emissions, on the path to the Paris agreement. Rev. Geophys. 58 (1), 1–51. https://doi.org/10.1029/2019RG000675.
Pasquill, F., 1961. The estimation of the dispersion of windborne material. Meteorol. Mag. 90, 33–49.
Phillips, N.G., Ackley, R., Crosson, E.R., Down, A., Hutyra, L.R., Brondfield, M., Karr, J. D., Zhao, K., Jackson, R.B., 2013. Mapping urban pipeline leaks: methane leaks across Boston. Environ. Pollut. 173, 1–4. https://doi.org/10.1016/j.envpol.2012.11.003.
PHMSA, 2022. SIGNIFICANT INCIDENT 20 YEAR TREND. Available at: Accessed 24 Apr 2022.
Ravikumar, A.P., Sreedhara, S., Wang, J., Englander, J., Roda-Stuart, D., Bell, C., Zimmerle, D., Lyon, D., Mogstad, I., Ratner, B., Brandt, A.R., 2019. Single-blind inter-comparison of methane detection technologies – results from the Stanford/EDF Mobile Monitoring Challenge. Elem Sci Anthr 7. https://doi.org/10.1525/elementa.373.
Ravikumar, A.P., Wang, J., McGuire, M., Bell, C.S., Zimmerle, D., Brandt, A.R., 2018. Good versus good enough?" Empirical tests of methane leak detection sensitivity of a commercial infrared camera. Environ. Sci. Technol. 52 (4), 2368–2374. https://doi.org/10.1021/acs.est.7b04945.
Rella, C.W., Tsai, T.R., Botkin, C.G., Crosson, E.R., Steele, D., 2015. Measuring emissions from oil and natural gas well pads using the mobile flux plane technique. Environ. Sci. Technol. 49 (7), 4742–4748. https://doi.org/10.1021/acs.est.5b00099.
Riddick, S.N., Bell, C.S., Duggan, A., Vaughn, T.L., Smits, K.M., Cho, Y., Bennett, K.E., Zimmerle, D.J., 2021. Modeling temporal variability in the surface expression above a methane leak: the ESCAPE model. J. Nat. Gas Sci. Eng. 96, 104275 https://doi.org/10.1016/j.jngse.2021.104275.
Riddle, A., Carruthers, D., Sharpe, A., McHugh, C., Stocker, J., 2004. Comparisons between FLUENT and ADMS for atmospheric dispersion modelling. Atmos. Environ. 38 (7), 1029–1038. https://doi.org/10.1016/j.atmosenv.2003.10.052.
Schivley, G., Azevedo, I., Samaras, C., 2018. Assessing the evolution of power sector carbon intensity in the United States. Environ. Res. Lett. 13 (6) https://doi.org/10.1088/1748-9326/aabe9d.
Sherwin, E.D., Chen, Y., Ravikumar, A.P., Brandt, A.R., 2021. Single-blind test of airplane-based hyperspectral methane detection via controlled releases. Elementa 9 (1), 1–10. https://doi.org/10.1525/elementa.2021.00063.
Stull, R.B., 2012. An Introduction to Boundary Layer Meteorology, vol. 13. Springer Science & Business Media.
Thorpe, A.K., Frankenberg, C., Aubrey, A.D., Roberts, D.A., Nottrott, A.A., Rahn, T.A., Sauer, J.A., Dubey, M.K., Costigan, K.R., Arata, C., Steffke, A.M., Hills, S., Haselwimmer, C., Charlesworth, D., Funk, C.C., Green, R.O., Lundeen, S.R., Boardman, J.W., Eastwood, M.L., et al., 2016. Mapping methane concentrations from a controlled release experiment using the next generation airborne visible/infrared imaging spectrometer (AVIRIS-NG). Remote Sens. Environ. 179, 104–115. https://doi.org/10.1016/j.rse.2016.03.032. Elsevier Inc.
Tian, S., Smits, K.M., Cho, Y., Riddick, S., Zimmerle, D., Duggan, A., 2022. Estimating Methane Emissions from Underground Natural Gas Pipelines Using an Atmospheric Dispersion-Based Method.
U.S. Energy Information Administration, 2021. Natural Gas Explained: Natural Gas Pipelines. Available at: Accessed 2 May 2022.
U.S. Energy Information Administration, 2022. Annual U.S. Natural Gas Production (1940-2020. Available at: Accessed 27 May 2022.
U.S. EPA, 2022. Inventory of U.S. Greenhouse Gas Emissions and Sinks: 1990-2020. Available at: Accessed 27 May 2022.
Ulrich, B.A., Mitton, M., Lachenmeyer, E., Hecobian, A., Zimmerle, D., Smits, K.M., 2019. Natural gas emissions from underground pipelines and implications for leak detection. Environ. Sci. Technol. Lett. 6 (7), 401–406. https://doi.org/10.1021/acs.estlett.9b00291.
UNFCCC, 2022. The Paris Agreement. Available at: Accessed 2 May 2022.
Weller, Z.D., Hamburg, S.P., Fischer, Von, 2020. A national estimate of methane leakage from pipeline mains in natural gas local distribution systems. Environ. Sci. Technol. 54 (14), 8958–8967. https://doi.org/10.1021/acs.est.0c00437.
Weller, Z.D., Roscioli, J.R., Daube, W.C., Lamb, B.K., Ferrara, T.W., Brewer, P.E., Fischer, Von, 2018. Vehicle-based methane surveys for finding natural gas leaks and estimating their size: validation and uncertainty. Environ. Sci. Technol. 52 (20), 11922–11930. https://doi.org/10.1021/acs.est.8b03135.
Zhang, J., Meerman, H., Benders, R., Faaij, A., 2022. Potential role of natural gas infrastructure in China to supply low-carbon gases during 2020–2050. Appl. Energy 306 (December 2020). https://doi.org/10.1016/j.apenergy.2021.117989.
Zhang, X., Myhrvold, N.P., Hausfather, Z., Caldeira, K., 2016. Climate benefits of natural gas as a bridge fuel and potential delay of near-zero energy systems. Appl. Energy 167, 317–322. https://doi.org/10.1016/j.apenergy.2015.10.016. Elsevier Ltd.
Zimmerle, D.J., Pickering, C.K., Bell, C.S., Heath, G.A., Nummedal, D., Pétron, G., Vaughn, T.L., 2017. Gathering pipeline methane emissions in Fayetteville shale pipelines and scoping guidelines for future pipeline measurement campaigns. Elem Sci Anth 5, 70. https://doi.org/10.1525/elementa.258.
Zimmerle, D, Vaughn, T, Bell, C, Bennett, K, Deshmukh, P, Thoma, E, 2020. Detection Limits of Optical Gas Imaging for Natural Gas Leak Detection in Realistic Controlled Conditions. Environ. Sci. Technol. 54 (18), 11506–11514. https://doi.org/10.1021/acs.est.0c01285.
Zou, C., Zhao, Q., Chen, J., Li, J., Yang, Z., Sun, Q., Lu, J., Zhang, G., 2018. Natural gas in China: development trend and strategic forecast. Nat. Gas. Ind. B 5 (4), 380–390. https://doi.org/10.1016/j.ngib.2018.04.010. Elsevier Ltd.